Dynamics of a System of Two Coupled Oscillators Driven by a Third Oscillator

Lauren Lazarus[1][†] and Richard H. Rand[2]

[1] Department of Mechanical and Aerospace Engineering, Cornell University, Ithaca, NY 14853, USA
[2] Department of Mathematics, Department of Mechanical and Aerospace Engineering, Cornell University, Ithaca, NY 14853, USA

Abstract

Analytical and numerical methods are applied to a pair of coupled nonidentical phase-only oscillators, where each is driven by the same independent third oscillator. The presence of numerous bifurcation curves defines parameter regions with 2, 4, or 6 solutions corresponding to phase locking. In all cases, only one solution is stable. Elsewhere, phase locking to the driver does not occur, but the average frequencies of the drifting oscillators are in the ratio of $m : n$. These behaviors are shown analytically to exist in the case of no coupling, and are identified using numerical integration when coupling is included.

1 Introduction

Recent experiments in optical laser MEMs have involved models of two coupled oscillators, each of which is being driven by a common harmonic forcer in the form of light [1]. Various steady states have been observed, including complete synchronization, in which both oscillators operate at the same frequency as the forcer, and partial synchronization, in which only one of the oscillators operates at the forcing frequency. Other possible steady states may exist, for example where the two oscillators are mutually synchronized but operate at a different frequency (or related frequencies) than that of the forcer ("relative locking"). Additionally, the oscillators may operate at frequencies unrelated to each other or to the forcing frequency ("drift"). The question of which of these various steady states is achieved will depend upon both the frequencies of the individual uncoupled oscillators relative to the forcing frequency, as well as upon the nature and strength of the forcing and of the coupling between the two oscillators.

Related studies have been done for other variants of the three coupled oscillator problem. Mendelowitz et al. [2] discussed a case with one-way coupling between the oscillators in a loop; this system resulted in two steady states due to choice of direction around the loop. Baesens et al. [3] studied the general three–oscillator system (all coupling patterns considered), provided the coupling was not too

---

[†] Corresponding author.
Email address: ll479@cornell.edu

strong, by means of maps of the two–torus.

Cohen et al. [4] modeled segments of neural networks as coupled limit cycle oscillators and discussed the special case of two coupled phase–only oscillators as described by the following:

$$\dot{\theta}_1 = \omega_1 + \alpha \, \sin(\theta_2 - \theta_1), \tag{1}$$
$$\dot{\theta}_2 = \omega_2 + \alpha \, \sin(\theta_1 - \theta_2). \tag{2}$$

Defining a new variable $\psi = \theta_2 - \theta_1$, being the phase difference between the two oscillators, allows the state of the system to be consolidated into a single equation:

$$\dot{\psi} = \omega_2 - \omega_1 - 2\alpha \, \sin\psi. \tag{3}$$

This is solved for an equilibrium point (constant ψ) which represents phase locking, i.e. the two oscillators traveling at the same frequency with some constant separation. This also gives us a constraint on the parameters which allow for phase locking to occur. If no equilibrium point exists, the oscillators will drift relative to each other; while they are affected by each other's phase, the coupling is not strong enough to compensate for the frequency difference.

$$\sin\psi^* = \frac{\omega_2 - \omega_1}{2\alpha}, \tag{4}$$
$$\left| \frac{\omega_2 - \omega_1}{2\alpha} \right| \leq 1. \tag{5}$$

Under the constraint, there are two possible equilibria ψ^* and $(\pi - \psi^*)$ within the domain, though one of them is unstable given that

$$\frac{d\dot{\psi}}{d\psi} = -2\alpha \, \cos\psi = -2\alpha(-\cos(\pi - \psi^*)).$$

So if one of them is stable $(d\dot{\psi}/d\psi < 0)$, the other must be unstable (and vice versa).

Plugging the equilibrium back into the original equations we find the frequency at which the oscillators end up traveling; this is a "compromise" between their respective frequencies.

$$\dot{\theta}_1 = \omega_1 + \alpha(\frac{\omega_2 - \omega_1}{2\alpha}) = \frac{\omega_1 + \omega_2}{2}. \tag{6}$$

Since the coupling strength is the same in each direction, the resultant frequency is an average of the two frequencies with equal weight; with different coupling strengths this would become a weighted average.

Keith and Rand [5] added coupling terms of the form $\alpha_2 \sin(\theta_1 - 2\theta_2)$ to this model and correspondingly found 2:1 locking as well as 1:1 locking.

2 Model

We design our model, as an extension of the two–oscillator model, to include a pair of coupled phase-only oscillators with a third forcing oscillator, as follows:

$$\dot{\theta}_1 = \omega_1 + \alpha \, \sin(\theta_2 - \theta_1) - \beta \, \sin(\theta_1 - \theta_3), \tag{7}$$
$$\dot{\theta}_2 = \omega_2 + \alpha \, \sin(\theta_1 - \theta_2) - \beta \, \sin(\theta_2 - \theta_3), \tag{8}$$
$$\dot{\theta}_3 = \omega_3. \tag{9}$$

This system can be related back to previous work by careful selection of parameters. Note that the $\beta = 0$ case reduces the system to two coupled oscillators without forcing, while $\alpha = 0$ gives a pair of uncoupled forced oscillators.

It is now useful to shift to a coordinate system based off of the angle of the forcing oscillator, since its frequency is constant. Let $\phi_1 = \theta_1 - \theta_3$ and $\phi_2 = \theta_2 - \theta_3$, with similar relations $\Omega_1 = \omega_1 - \omega_3$ and $\Omega_2 = \omega_2 - \omega_3$ between the frequencies. The forcing oscillator's equation of motion can thus be dropped.

$$\dot{\phi}_1 = \Omega_1 + \alpha \ \sin(\phi_2 - \phi_1) - \beta \ \sin \phi_1, \tag{10}$$

$$\dot{\phi}_2 = \Omega_2 + \alpha \ \sin(\phi_1 - \phi_2) - \beta \ \sin \phi_2. \tag{11}$$

A nondimensionalization procedure, scaling time with respect to Ω_1, allows for $\Omega_1 = 1$ to be assumed without loss of generality.

We note that the ϕ_i now represent phase *differences* between the paired oscillators and the driver. Thus, if a $\dot{\phi}_i = 0$, the corresponding θ_i is defined to be locked to the driver. Equilibrium points of equations (10) and (11) then represent full locking of the system. Partial and total drift are more difficult to recognize and handle analytically, and will be discussed later.

3 Full Locking

We begin by solving the differential equations for equilibria directly, so as to find the regions of parameter space for which the system locks to the driver. The equilibria satisfy the equations:

$$0 = 1 + \alpha \ \sin(\phi_2 - \phi_1) - \beta \ \sin \phi_1, \tag{12}$$

$$0 = \Omega_2 + \alpha \ \sin(\phi_1 - \phi_2) - \beta \ \sin \phi_2. \tag{13}$$

Trigonometrically expanding equation (12) and solving for $\cos \phi_1$:

$$\cos \phi_1 = \frac{\alpha \ \sin \phi_1 \ \cos \phi_2 + \beta \ \sin \phi_1 - 1}{\alpha \ \sin \phi_2}. \tag{14}$$

We square this equation, rearrange it, and use $\sin^2 \theta + \cos^2 \theta = 1$ to replace most cosine terms:

$$\begin{aligned} &\alpha^2 \ (1 - \sin^2 \ \phi_1) \ \sin^2 \ \phi_2 \\ &- \alpha^2 \ \sin^2 \ \phi_1 (1 - \sin^2 \ \phi_2) \\ +&(2\alpha \ \sin \phi_1 - 2\alpha\beta \ \sin^2 \ \phi_1) \ \cos \phi_2 \\ &- \beta^2 \ \sin^2 \ \phi_1 + 2\beta \ \sin \phi_1 - 1 = 0. \end{aligned} \tag{15}$$

Repeating the process by solving for $\cos \phi_2$, we obtain an equation in terms of only sines:

$$\begin{aligned} -[4\alpha^2\beta^2 \ \sin^4 \ \phi_1 - 8\alpha^2\beta \ \sin^3 \ \phi_1 \\ + (4\alpha^2 - 2\alpha^2\beta^2 - 2\alpha^4) \ \sin^2 \ \phi_1 \\ + 4\alpha^2\beta \ \sin \phi_1 - 2\alpha^2] \ \sin^2 \ \phi_2 \\ -\alpha^4 \ \sin^4 \ \phi_2 - (\beta^4 - 2\alpha^2\beta^2 + \alpha^4) \ \sin^4 \ \phi_1 \\ -(4\alpha^2\beta - 4\beta^3) \ \sin^3 \ \phi_1 - (6\beta^2 - 2\alpha^2) \ \sin^2 \ \phi_1 \\ + 4\beta \ \sin \phi_1 - 1 = 0. \end{aligned} \tag{16}$$

Returning to equations (12) and (13), we add them and solve for $\sin \phi_2$ in terms of $\sin \phi_1$:

$$\sin \phi_2 = \frac{1 + \Omega_2}{\beta} - \sin \phi_1. \tag{17}$$

This is now plugged into equation (16) to eliminate ϕ_2 and obtain an polynomial of degree six in $s = \sin \phi_1$, dependent on the various parameters.

$$
\begin{aligned}
&-4\alpha^2\beta^6 s^6 + 8\alpha^2\beta^5\Omega_2 s^5 + 16\alpha^2\beta^5 s^5 - 24\alpha^2\beta^4\Omega_2 s^4 - \beta^8 s^4 + 4\alpha^2\beta^6 s^4 - 24\alpha^2\beta^4 s^4 \\
&-4\alpha^2\beta^4\Omega_2^2 s^4 + 8\alpha^2\beta^3\Omega_2^2 s^3 - 4\alpha^2\beta^5\Omega_2 s^3 + 24\alpha^2\beta^3\Omega_2 s^3 + 4\beta^7 s^3 - 12\alpha^2\beta^5 s^3 \\
&+16\alpha^2\beta^3 s^3 + 2\alpha^2\beta^4\Omega_2^2 s^2 - 4\alpha^4\beta^2\Omega_2^2 s^2 - 4\alpha^2\beta^2\Omega_2^2 s^2 + 12\alpha^2\beta^4\Omega_2 s^2 - 8\alpha^4\beta^2\Omega_2 s^2 \\
&-8\alpha^2\beta^2\Omega_2 s^2 - 6\beta^6 s^2 + 14\alpha^2\beta^4 s^2 - 4\alpha^4\beta^2 s^2 - 4\alpha^2\beta^2 s^2 + 4\alpha^4\beta\Omega_2^3 s - 4\alpha^2\beta^3\Omega_2^2 s \\
&+12\alpha^4\beta\Omega_2^2 s - 12\alpha^2\beta^3\Omega_2 s + 12\alpha^4\beta\Omega_2 s + 4\beta^5 s - 8\alpha^2\beta^3 s + 4\alpha^4\beta s - \alpha^4\Omega_2^4 - 4\alpha^4\Omega_2^3 \\
&+2\alpha^2\beta^2\Omega_2^2 - 6\alpha^4\Omega_2^2 + 4\alpha^2\beta^2\Omega_2 - 4\alpha^4\Omega_2 - \beta^4 + 2\alpha^2\beta^2 - \alpha^4 = 0. \qquad (18)
\end{aligned}
$$

The roots of this polynomial give values of $s = \sin \phi_1$ for a given set of parameter values; degree six implies that there will be up to six roots in s, although a single root in s may correspond to more than one root in ϕ_1 due to the multivalued nature of sine. To avoid extraneous roots, each should be confirmed in equations (12) and (13).

In order to distinguish changes in the number of real equilibria, we look for double roots of this polynomial such that two (or more) of the equilibria are coalescing in a single location. Setting the polynomial and its derivative in s equal to zero and using Maxima to eliminate s results in a single equation with 142 terms in α, β, and Ω_2 which describes the location of bifurcations.

$$
\begin{aligned}
&48\Omega_2^8\alpha^4\beta^4 - 360\Omega_2^8\alpha^6\beta^2 - 32\Omega_2^8\alpha^4\beta^2 - 87\Omega_2^8\alpha^8 + 64\Omega_2^{10}\alpha^6 + 320\Omega_2^9\alpha^6 - 128\Omega_2^7\alpha^4\beta^4 \\
&-1308\Omega_2^7\alpha^6\beta^2 - 112\Omega_2^7\alpha^4\beta^2 - 160\Omega_2^7\alpha^8 + 616\Omega_2^8\alpha^6 + 16\Omega_2^8\alpha^4 + 12\Omega_2^6\alpha^2\beta^8 + 22\Omega_2^6\alpha^4\beta^6 \\
&-16\Omega_2^6\alpha^2\beta^6 + 410\Omega_2^6\alpha^6\beta^4 + 528\Omega_2^7\alpha^6 + 64\Omega_2^7\alpha^4 + 6\Omega_2^6\alpha^4\beta^4 + 8\Omega_2^6\alpha^2\beta^4 + 140\Omega_2^6\alpha^8\beta^2 \\
&-1720\Omega_2^6\alpha^6\beta^2 - 224\Omega_2^6\alpha^4\beta^2 + 256\Omega_2^6\alpha^{10} - 52\Omega_2^5\alpha^2\beta^8 + 324\Omega_2^5\alpha^4\beta^6 + 100\Omega_2^5\alpha^2\beta^6 \\
&+796\Omega_2^6\alpha^8 + 88\Omega_2^6\alpha^6 + 96\Omega_2^6\alpha^4 + 1952\Omega_2^5\alpha^6\beta^4 + 448\Omega_2^5\alpha^4\beta^4 - 48\Omega_2^5\alpha^2\beta^4 - 1240\Omega_2^5\alpha^8\beta^2 \\
&-996\Omega_2^5\alpha^6\beta^2 - 288\Omega_2^5\alpha^4\beta^2 + \Omega_2^4\beta^{12} - 34\Omega_2^4\alpha^2\beta^{10} + 1536\Omega_2^5\alpha^{10} + 3232\Omega_2^5\alpha^8 \\
&-160\Omega_2^5\alpha^6 + 64\Omega_2^5\alpha^4 - 2\Omega_2^4\beta^{10} - 189\Omega_2^4\alpha^4\beta^8 + 54\Omega_2^4\alpha^2\beta^8 + \Omega_2^4\beta^8 - 480\Omega_2^4\alpha^6\beta^6 \\
&+94\Omega_2^4\alpha^4\beta^6 - 40\Omega_2^4\alpha^2\beta^6 + 960\Omega_2^4\alpha^8\beta^4 + 1526\Omega_2^4\alpha^6\beta^4 + 404\Omega_2^4\alpha^4\beta^4 + 8\Omega_2^4\alpha^2\beta^4 \\
&-1024\Omega_2^4\alpha^{10}\beta^2 - 6284\Omega_2^4\alpha^8\beta^2 - 448\Omega_2^4\alpha^6\beta^2 - 224\Omega_2^4\alpha^4\beta^2 + 3840\Omega_2^4\alpha^{10} + 4726\Omega_2^4\alpha^8 \\
&+88\Omega_2^4\alpha^6 + 108\Omega_2^3\alpha^2\beta^{10} - 152\Omega_2^3\alpha^4\beta^8 - 208\Omega_2^3\alpha^2\beta^8 + 16\Omega_2^4\alpha^4 - 752\Omega_2^3\alpha^4\beta^6 \\
&+100\Omega_2^3\alpha^2\beta^6 + 2560\Omega_2^3\alpha^8\beta^4 + 48\Omega_2^3\alpha^6\beta^6 - 96\Omega_2^3\alpha^6\beta^4 + 448\Omega_2^3\alpha^4\beta^4 - 4096\Omega_2^3\alpha^{10}\beta^2 \\
&-9808\Omega_2^3\alpha^8\beta^2 - 996\Omega_2^3\alpha^6\beta^2 - 112\Omega_2^3\alpha^4\beta^2 + 5120\Omega_2^3\alpha^{10} + 3232\Omega_2^3\alpha^8 + 528\Omega_2^3\alpha^6 \\
&-2\Omega_2^2\beta^{14} + 30\Omega_2^2\alpha^2\beta^{12} + 68\Omega_2^2\alpha^4\beta^{10} - 56\Omega_2^2\alpha^2\beta^{10} - 2\Omega_2^2\beta^{10} - 320\Omega_2^2\alpha^6\beta^8 \\
&-166\Omega_2^2\alpha^4\beta^8 + 54\Omega_2^2\alpha^2\beta^8 + 512\Omega_2^2\alpha^8\beta^6 + 864\Omega_2^2\alpha^6\beta^6 + 94\Omega_2^2\alpha^4\beta^6 - 16\Omega_2^2\alpha^2\beta^6 \\
&+3200\Omega_2^2\alpha^8\beta^4 + 1526\Omega_2^2\alpha^6\beta^4 + 6\Omega_2^2\alpha^4\beta^4 - 6144\Omega_2^2\alpha^{10}\beta^2 - 6284\Omega_2^2\alpha^8\beta^2 - 1720\Omega_2^2\alpha^6\beta^2 \\
&-56\Omega_2\alpha^2\beta^{12} + 152\Omega_2\alpha^4\beta^{10} - 32\Omega_2^2\alpha^4\beta^2 + 3840\Omega_2^2\alpha^{10} + 4\Omega_2^2\beta^{12} + 796\Omega_2^2\alpha^8 \\
&+616\Omega_2^2\alpha^6 + 108\Omega_2\alpha^2\beta^{10} - 152\Omega_2\alpha^4\beta^8 - 52\Omega_2\alpha^2\beta^8 + 1024\Omega_2\alpha^8\beta^6 + 48\Omega_2\alpha^6\beta^6 \\
&+324\Omega_2\alpha^4\beta^6 + 2560\Omega_2\alpha^8\beta^4 + 1952\Omega_2\alpha^6\beta^4 - 128\Omega_2\alpha^4\beta^4 - 832\Omega_2\alpha^6\beta^8 - 4096\Omega_2\alpha^{10}\beta^2 \\
&-1240\Omega_2\alpha^8\beta^2 + \beta^{16} - 12\alpha^2\beta^{14} - 1308\Omega_2\alpha^6\beta^2 + 1536\Omega_2\alpha^{10} - 160\Omega_2\alpha^8 \\
&+320\Omega_2\alpha^6 - 2\beta^{14} + 48\alpha^4\beta^{12} + 30\alpha^2\beta^{12} + \beta^{12} - 64\alpha^6\beta^{10} + 68\alpha^4\beta^{10} \\
&-34\alpha^2\beta^{10} - 320\alpha^6\beta^8 - 189\alpha^4\beta^8 + 12\alpha^2\beta^8 + 512\alpha^8\beta^6 - 480\alpha^6\beta^6 + 22\alpha^4\beta^6 + 960\alpha^8\beta^4 \\
&+410\alpha^6\beta^4 + 48\alpha^4\beta^4 - 1024\alpha^{10}\beta^2 + 140\alpha^8\beta^2 - 360\alpha^6\beta^2 + 256\alpha^{10} - 87\alpha^8 + 64\alpha^6 = 0. \quad (19)
\end{aligned}
$$

This equation by itself is cumbersome to work with. We begin to interpret its results by choosing different values of Ω_2 and plotting the resulting curves in the $\beta\alpha$-plane (see Fig. 1). Each curve is
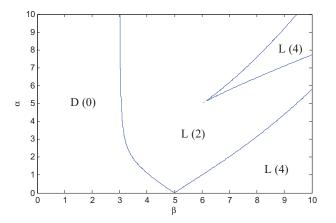
Fig. 1 $\Omega_2 = 5$ cross-section of surfaces satisfying equation (19). Regions show "L" for locking or "D" for drift, followed by number of equilibria.
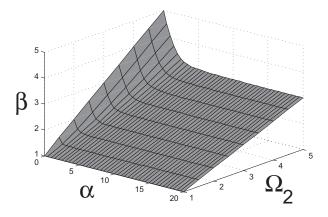

Fig. 2 Surface of double roots forming the boundary between complete synchronization and the other behaviors.

the location of a double root of the original system, and represents a pair of equilibrium points being created or destroyed in a fold bifurcation. The combination of bifurcation curves leads to regions of 0–6 equilibria.

Numerical analysis of the original differential equations with AUTO continuation software [6] both confirms the quantities of equilibria and calculates the eigenvalues of each point. Through these results, we find that only one equilibrium point (and therefore locking behavior) is stable; it occurs for any region where equilibria exist, i.e. for large enough forcing strength β.

The leftmost curve, where the first two equilibria are created, is of most interest since it is the boundary between drift and total locking. Figure 2 shows only this surface in three dimensions.

3.1 Asymptotics

Asymptotic expansions of equation (19) may be useful for very large or very small α, in applications where the entire equation would be cumbersome. For these purposes, we assume that $\Omega_2 \geq \Omega_1 = 1$; if this is not true, the two oscillators' labels can switch such that this analysis is applicable.
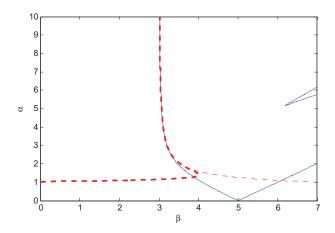
Fig. 3 Approximations for large α: dashed line accurate to $O(\alpha^{-4})$, bold dashed line to $O(\alpha^{-8})$. $\Omega_2 = 5$.

3.1.1 Large α Approximation

For large α the curve appears to approach a constant value β. We divide by the highest power, α^{10}, in equation (19), then take the limit as α goes to infinity to find that the equation approaches:

$$256 \, (\Omega_2 + 1)^4 \, (\Omega_2 - 2\beta + 1) \, (\Omega_2 + 2\beta + 1) = 0. \tag{20}$$

The middle portion can equal zero for $\Omega_2 \geq 1$, leading to the asymptotic value of β:

$$\beta = \frac{1 + \Omega_2}{2}. \tag{21}$$

We perturb off of this value by writing β as:

$$\beta = \frac{1 + \Omega_2}{2} + \frac{k_1}{\alpha} + \frac{k_2}{\alpha^2} + \cdots \tag{22}$$

The k_i for odd i are found to be zero, leaving an expression for β with only even terms.

$$\beta = \frac{1}{2}(\Omega_2 + 1) + \frac{1}{64\alpha^2}(\Omega_2 - 1)^2(\Omega_2 + 1) \tag{23}$$
$$+ \frac{7}{4096\alpha^4}(\Omega_2 - 1)^4(\Omega_2 + 1)$$
$$+ \frac{(25\Omega_2^2 - 82\Omega_2 + 25)}{131072\alpha^6}(\Omega_2 - 1)^4(\Omega_2 + 1) + \cdots$$

We note that there is a common factor of $(\Omega_2 + 1)/2$ present in all terms, which acts as an overall scaling factor for the expression. Figure 3 compares this approximation out to 3 and 5 terms in $1/\alpha^2$ with the original numerical result.

3.1.2 Small α Approximation

In the $\alpha = 0$ case, the algebraic equations to be solved, eqs. (12) and (13), become uncoupled:

$$0 = 1 - \beta \, \sin\phi_1, \tag{24}$$
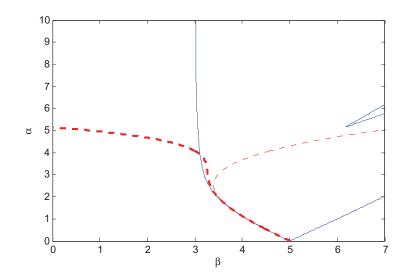$$0 = \Omega_2 - \beta \, \sin\phi_2. \tag{25}$$

Fig. 4 Approximations for small α: dashed line accurate to $O(\alpha^4)$, bold dashed line to $O(\alpha^7)$. $\Omega_2 = 5$.

In order for both to have real solutions, $\beta \geq 1$ and $\beta \geq \Omega_2$ must both be satisfied. Thus, under our assumption that $\Omega_2 \geq 1$, equilibria (and therefore locking behavior) will exist for $\beta \geq \Omega_2$.

We perturb off of $\beta = \Omega_2$ for small α in equation (19):

$$\beta = \Omega_2 + \mu_1 \alpha + \mu_2 \alpha^2 + \cdots \tag{26}$$

This leads to two different branches, differentiated by the sign of the μ_1 term, due to the intersection of the drift/lock boundary with another bifurcation curve at $\alpha = 0$. Choosing the drift/lock boundary by taking the negative μ_1 such that β decreases for positive α:

$$\begin{aligned}
\beta = \Omega_2 &- \frac{\sqrt{\Omega_2^2 - 1}}{\Omega_2} \alpha + \frac{(2\Omega_2 + 1)}{2\Omega_2^3} \alpha^2 \\
&+ \frac{(\Omega_2^4 + 2\Omega_2^3 - \Omega_2^2 - 2\Omega_2 - 1)}{2\Omega_2^5 \sqrt{\Omega_2^2 - 1}} \alpha^3 \\
&+ \frac{(4\Omega_2^6 - 12\Omega_2^4 - 12\Omega_2^3 - \Omega_2^2 + 12\Omega_2 + 5)}{8(\Omega_2 - 1)\Omega_2^7(\Omega_2 + 1)} \alpha^4 \ldots
\end{aligned} \tag{27}$$

Figure 4 shows this approximation out to 5 and 8 terms in α.

3.1.3 Patched Solution: A Practical Approximation

We approximate the lock/drift boundary curve by two lines for different ranges of α based on their intersection. Our two approximations, taken to be linear:

$$\beta = \frac{1}{2}(\Omega_2 + 1) + O(\alpha^{-2}) \tag{28}$$

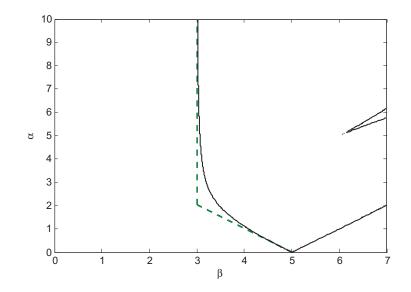$$\beta = \Omega_2 - \frac{\sqrt{\Omega_2^2 - 1}}{\Omega_2} \alpha + O(\alpha^2) \tag{29}$$

Fig. 5 Linear piecewise approximation for the drift/lock boundary. $\Omega_2 = 5$.

Ignoring nonlinear terms and finding the intersection (β^*, α^*) for a given Ω_2,

$$\beta^* = \Omega_2 - \frac{\sqrt{\Omega_2^2 - 1}}{\Omega_2} \qquad \alpha^* = \frac{1}{2}(\Omega_2 + 1) \tag{30}$$

$$\alpha^* = \frac{\Omega_2(\Omega_2 - 1)}{2\sqrt{\Omega_2^2 - 1}} = \frac{\sqrt{\beta^* - 1}(2\beta^* - 1)}{2\sqrt{\beta^*}} \tag{31}$$

Then we can consider the combined linear approximation to be the piecewise function for β with eq. (29) for $\alpha \leq \alpha^*$ and eq. (28) for $\alpha \geq \alpha^*$. See Fig. 5.

4 The Drift Region

Within the region of no equilibrium points, we can study different forms of drift: full drift, m:n relative locking between the ϕ_i while drifting with respect to the driver, or partial synchronization with one oscillator locked to the driver (while the other drifts). To distinguish between these, we start by separately considering the cases $\beta = 0$ and $\alpha = 0$. See Fig. 6.

4.1   No Driver $\beta = 0$

We begin with the system with no driver, $\beta = 0$ (as addressed by Cohen et al. [4], see introduction):

$$\dot{\psi} = \frac{d}{dt}(\phi_2 - \phi_1) = \Omega_2 - \Omega_1 - 2\alpha \sin \psi$$

and observe that ϕ_1 and ϕ_2 experience 1:1 phase locking for

$$\alpha \geq |\Omega_2 - 1|/2$$

but there is no locking to θ_3. Thus, corroborating intuition, stronger coupling (larger values of α) results in $1:1$ locking. We would anticipate that this behavior would extend (for nonzero β) into the
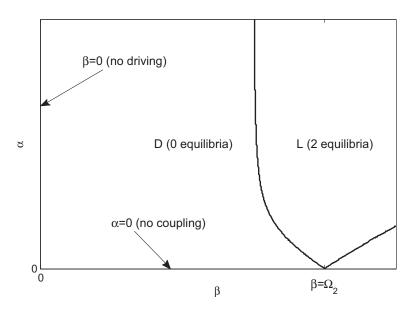
Fig. 6 Locations of interest for analytical approaches to the drift region.

large$-\alpha$ realm of parameter space, before the driver is strong enough to cause phase locking.

4.2 No Coupling $\alpha = 0$

Next, we consider the $\alpha = 0$ case, since the two ϕ_i differential equations become uncoupled and can thus be individually integrated. By separation of variables, we find:

$$dt = \frac{d\phi_1}{1 - \beta \sin \phi_1} = \frac{d\phi_2}{\Omega_2 - \beta \sin \phi_2}, \tag{32}$$

which can be integrated to find:

$$t(\phi_i) + C_i = 2Q_i \tan^{-1} [Q_i(\frac{\Omega_i \sin \phi_i}{\cos \phi_i + 1} - \beta)], \tag{33}$$

where

$$Q_i = 1/\sqrt{\Omega_i^2 - \beta^2}. \tag{34}$$

If we consider a full cycle of ϕ_i, that is, the domain $\phi_0 \leq \phi_i \leq 2\pi + \phi_0$, the argument of the arctangent covers its entire domain of $(-\infty, \infty)$ exactly once, so the entire range π of arctangent is covered exactly once. Thus the Δt_i corresponding to this $\Delta \phi_i$ is:

$$\Delta t_i = 2\pi Q_i = 2\pi/\sqrt{\Omega_i^2 - \beta^2}. \tag{35}$$

Given a known Ω_2 and choosing particular values of β, it should be possible to find a Δt which is an integer multiple of each of the two oscillators' periods. That is, $\Delta t = n_2 \Delta t_1 = n_1 \Delta t_2$ such that in that time, ϕ_1 travels $2\pi n_2$ and ϕ_2 travels $2\pi n_1$. Thus the oscillators would have motion with the ratio $n_1 : n_2$ between their average frequencies.

$$\frac{\Delta t_1}{\Delta t_2} = \frac{n_1}{n_2} = \frac{\sqrt{\Omega_2^2 - \beta^2}}{\sqrt{\Omega_1^2 - \beta^2}}. \tag{36}$$

By solving for β, we can then pick integers n_i and find the location on $\alpha = 0$ where that type of orbit occurs.

$$\beta^2 = \frac{\Omega_1^2 n_1^2 - \Omega_2^2 n_2^2}{n_1^2 - n_2^2}. \tag{37}$$

Note that this is not solvable for $n_1 = n_2 = 1$ unless the oscillators are the same and identically influenced by the driver ($\Omega_1 = \Omega_2$); this behavior is instead found on $\beta = 0$ as seen above.

Each ratio $n_1 : n_2$ will have a corresponding β_{n_2/n_1} for $\alpha = 0$; some example values are found in Tab. 1. It is reasonable to think that for small values of α near the β_{n_2/n_1}, the $n_1 : n_2$ behavior might persist although we are no longer able to study the oscillators separately.

Table 1   Example $n_1 : n_2$ locations on $\alpha = 0$ for $\Omega_2 = 1.1$

n_1	n_2	β_{n_2/n_1}
1	1	does not exist
2	1	0.9644
3	1	0.9868
3	2	0.9121
1	0	$\geq \Omega_1 = 1$

4.3   Numerical

Based on the $\alpha = 0$ and $\beta = 0$ cases, we expect to find regions of $n_1 : n_2$ relative locking continuing into the rest of the drift region. Through analysis of numerically computed solutions, we focused on cases of $N : 1$ behaviors, though our method should be applicable to more general cases with minor adjustments.

After allowing the system to reach a steady state, we integrate for a $\Delta\phi_1 = 2\pi$ and find the corresponding $\Delta\phi_2$. If this $\Delta\phi_2$ is an integer multiple of 2π, the point in parameter space is classified appropriately as $N : 1$; otherwise, it likely follows some other $n_1 : n_2$ ratio and is not shown. Alternately, if ϕ_1 is constant such that a corresponding $\Delta\phi_2$ would be arbitrary, the point is classified as $1 : 0$ or as an equilibrium.

The results for $0.91 \leq \beta \leq 1.1$, along with the drift/lock boundary curve from above, are shown in Fig. 7. (Note that Figs. 1-5 were calculated for $\Omega_2 = 5$, whereas Figs. 7 and 8 are for $\Omega_2 = 1.1$.) Some additional tongues were found numerically that also do not appear in the figure, as the higher $N : 1$ tongues are increasingly narrow. We also observe that beyond the edge of Fig. 7, the boundary of the $1 : 1$ relative locking region extends to $\alpha = 0.05$ for $\beta = 0$, as expected from our prior calculation.

As anticipated, we find that the tongues of $N : 1$ relative locking emerge from the analytically calculated values on the β axis. These tongues stretch across the $\beta\alpha$-plane and terminate when they reach the drift/lock bifurcation curve. Figure 8 zooms in on the region of termination; note that the tongues still have nontrivial width when they reach the bifurcation curve.

Figure 9 shows a schematic description of the termination of the tongues at the drift/lock bifurcation curve. Each $N : 1$ region disappears in the saddle-node bifurcation in which a pair of equilibria is born (one stable, one unstable), located on the other side of the bifurcation curve. Each $N : 1$ region in the sequence is separated from the next by a region which is filled with other $n_1 : n_2$ tongues.

As N increases, a limit is reached which corresponds to $1 : 0$ locking (i.e. $\infty : 1$). Within this region, ϕ_1 is locked to the driver, but ϕ_2 is not, representing partial synchronization to the driver (rather than relative locking between the oscillators). The curve bounding this region intersects the β axis at $\beta = \Omega_1 = 1$.
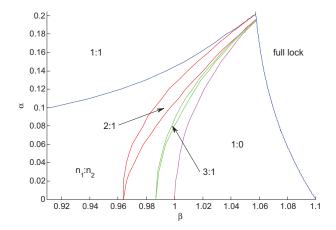
Fig. 7 $\Omega_2 = 1.1$; numerical $N:1$ findings and drift/lock bifurcation curve.
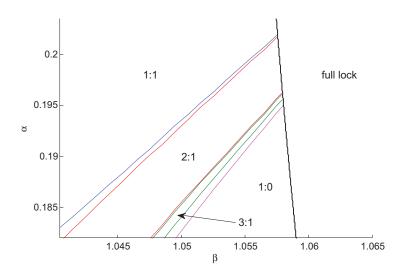

Fig. 8 Numerical $N:1$ findings and drift/lock boundary zoomed in. $\Omega_2 = 1.1$.

5 Conclusion

This work has approached a system of three coupled oscillators which represent a coupled pair under the same periodic external forcing. We investigated the existence of full locking behaviors between the oscillators, and presented two approximations for the boundary between drift and locking based on relative frequencies and coupling strengths. We also studied the various classifications of drift behavior, and their locations in parameter space, including various m:n resonances of the driven pair. In the latter case, the behavior of one oscillator relative to the other is periodic, but the observed behavior of the three-oscillator system is quasiperiodic due to drift relative to the driver.

This project was motivated by the consideration of a pair of coupled oscillators exposed to an environmental forcing. Further work may include the application of this analysis to more realistic models, such as the van der Pol oscillator, or an expanded set of parameters which could represent nonidentical coupling and driving strengths. Other appropriate considerations would involve the effect of the delay in this problem, or separate environmental drivers, which would both characterize nontrivial distance between the coupled pair of oscillators.
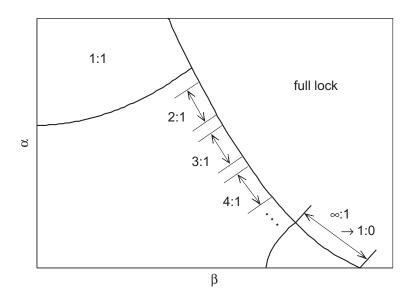
Fig. 9 Behaviors at the drift/lock boundary curve; not to scale.

Acknowledgements

References

[1] Zhang, M., Wiederhecker, G.S., Manipatruni, S., Barnard, A., McEuen, P., and Lipson, M. (2012), Synchronization of Micromechanical Oscillators Using Light, *Physical Review Letters*, **109** (23), 233906.
[2] Mendelowitz, L., Verdugo, A., and Rand, R. (2009), Dynamics of three coupled limit cycle oscillators with application to artificial intelligence, *Communications in Nonlinear Science and Numerical Simulation*, **14** (1), 270–283.
[3] Baesens, C., Guckenheimer, J., Kim, S., MacKay, R.S. (1991), Three coupled oscillators: mode–locking, global bifurcations and toroidal chaos, *Physica D*, **49** (3), 387–475.
[4] Cohen, A.H., Holmes, P.J., and Rand, R.H. (1982), The Nature of the Coupling Between Segmental Oscillators of the Lamprey Spinal Generator for Locomotion: A Mathematical Model, *Journal of Mathematical Biology*, **13** (3), 345-369.
[5] Keith, W. L. and Rand, R. H. (1984), 1:1 and 2:1 phase entrainment in a system of two coupled limit cycle oscillators, *J. Math. Biology*, **20** (2), 133–152.
[6] Doedel, E., Champneys, A., Fairgrieve, T., Kuznetsov, Y., Sandstede, B., Wang, X. (1998), AUTO 97: Continuation and Bifurcation Software for Ordinary Differential Equations.